Capability for B measurement – semileptonic decay channel for CDR

10k Hijing Au+Au 200 GeV central events are produced in full STAR environment with CD0 geometry (old) and w/o BTOF at this moment. The event vertex resolution in X-Y is 0.01 cm and with a Gaussian distribution of vertex Z with σz=20 cm, positing in ±5 cm from detector center. The reconstructed vertex resolution is ~3 μm in r-φ and z with HFT constraint, which provides the precision to distinguish the distance of closest approach to primary vertex (DCA) of the electrons from different heavy flavor mesons (D, B) semileptonic decays due to their different cτ, see Figure 1.

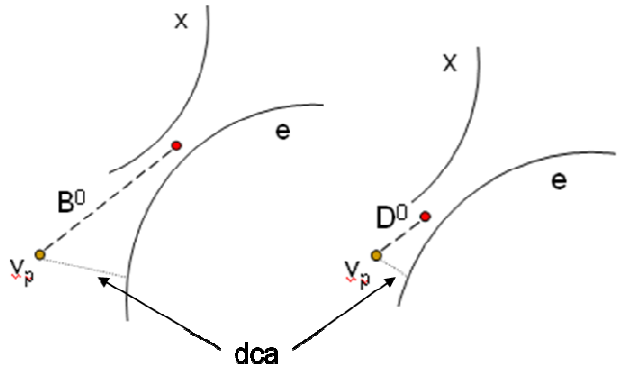

Figure 1: The difference of the DCA of daughter electrons from D^0 and B^0 semileptonic decays.

100 D^0, D^+, B^0, B^+ were embedded flat in p_T (0.2-20 GeV/c) in each event. The pseudo-rapidity is flat in ±1 and azimuthal angle is flat in 2π. The p_T spectra were weighted using STAR measured D^0 spectrum power-law distribution for D mesons and FONLL calculation for B mesons in later analysis. D^0 and D^+ decay to semileptonic channel (D^0, $D^+ \rightarrow$ e + X) with 100% branching ratio. B^0 and B^+ are very similar in this simulation, we use B represent both of them. B 75% decay to semileptonic channel (B → e + D* + X) and 25% decay to semileptonic channel (B → e + D + X). The fraction of the process B→D*→D→e is relatively small, we only simulate B→e + X and B→D→e. All these channels are later scaled by the fragmentation ratio (F.R.) and branching ratio (B.R.) in the analysis. Table 1 listed the cτ, mass, F.R. and B.R. for the particles.

particles	cτ (μm)	Mass (GeV/c^2)	q(c,b) → X (F.R.)	X → e (B.R.)
D^0	123	1.865	0.54	0.0671
D^+	312	1.869	0.21	0.172
B^0	459	5.279	0.40	0.104
B^+	491	5.279	0.40	0.109

Table 1: PDG numbers of D, B mesons.

Due to larger cτ, the DCA distribution of B → e was expected to be broader than

that of $D^0 \rightarrow$ e. Since D^+ $c\tau$ is more close to B mesons, it becomes a challenge to distinguish them by electron DCA distributions only. But the D^+ reconstruction via hadronic decay (e.g. $D^+ \rightarrow K\pi\pi$) can provide precise constraint on their decay electron p_T distributions. Thus together with the electron DCA distributions, we can separate D and B mesons with HFT.

The HFT has a good efficiency to measure electrons. Left panel of Figure 2 shows the electron tracking efficiencies with (blue circles, ~61%) or w/o (red and black circles, ~75%) pixel hits required. Right Panel shows the electron tracking efficiency (~60%) after p_T weighted for $D^0 \rightarrow$e. Here ~85% TPC tracking efficiency is included.

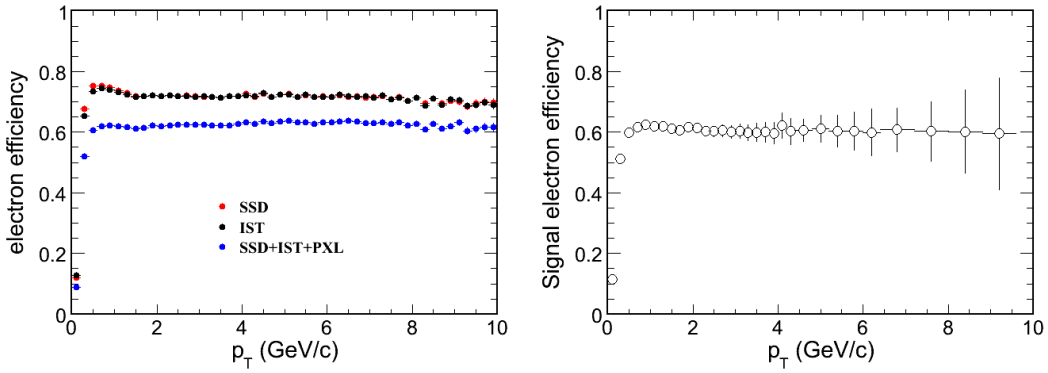

Figure 2: Efficiency of electron in the STAR TPC+HFT tracking.

Perfect PID was applied for electrons. Realistic PID by BTOF and *d*E/*d*x is in progress. The good electron candidate was selected with number of fit points > 15, pseudo-rapidity in $\pm$1, and with two pixel hits required.

Most of the photon converted electron outside of pixel detector can be removed due to their random large DCA distributions. The main background sources in this analysis are photon converted electron from beam pipe and electron from π^0, η Dalitz decays, the simulation on this part is in progress. Background from other hadron decays is small. Due to background statistics, we assume its p_T decreasing exponentially and extrapolated to high p_T. At high p_T, background is neglectable.

The electron DCA distributions from different decay processes were normalized by the corresponding F.R. and B.R., and total electron yield was normalized to STAR measured non-photonic electron (NPE) spectrum. (B$\rightarrow$e) / NPE ratio was normalized to fit STAR measured data (from e-h correlation). Figure 3 shows the electron DCA distributions at $2.4 < p_T < 3$ GeV/c (left panel) and at $4.8 < p_T < 5.4$ GeV/c (right panel) for $D^0 \rightarrow$e (red), $D^+ \rightarrow$e (green), B$\rightarrow$e (blue) and B$\rightarrow$D$\rightarrow$e (purple). The background from hijing events is shown as the dashed curve. The black solid curve presents the total electron DCA distribution, which was normalized to STAR measured NPE spectrum.

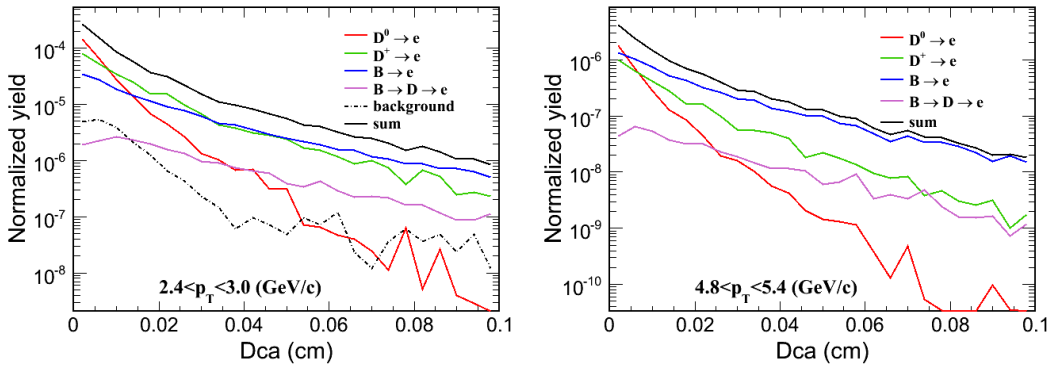

Figure 3: The electron DCA distributions for D, B meson semileptonic decays.

In real experimental data, we can use the different DCA distributions to fit the total DCA distribution to extract the raw yield of each source of electrons. The D meson p_T distributions from the measurement via hadronic decay channel will constrain the D⟶e distribution. By subtracting the D⟶e DCA distribution in each p_T bin from the total DCA distribution, the electron from B meson decays can be obtained.

From the dca distributions and the efficiency, the D⟶e, B⟶e and B⟶ D⟶e spectra can be obtained, and the statistical errors were estimated for 100M 200 GeV Au+Au central events (non-special trigger), shown in Figure 4.

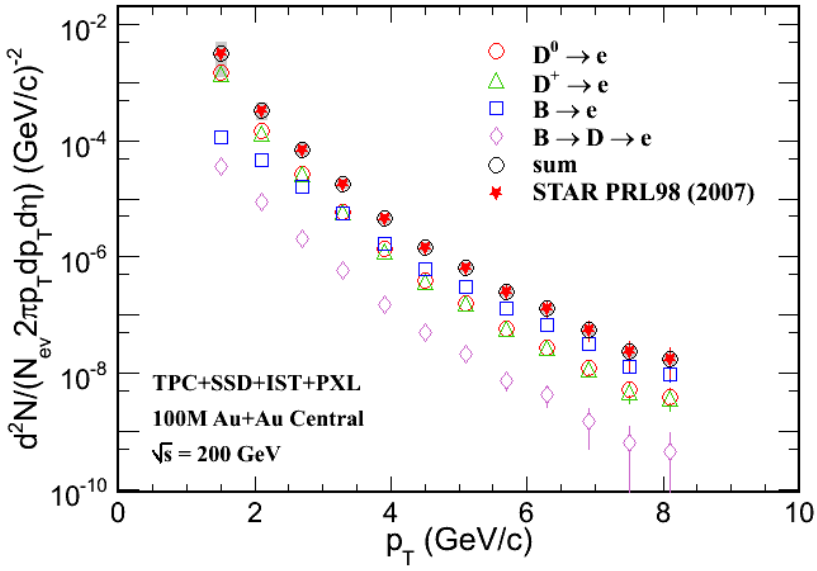

Figure 4: Electron spectra from B, D meson semileptonic decays. The expected errors as a function of p_T were estimated for 100M 200 GeV Au+Au central events.

The (B⟶e)/NPE ratio can be directly measured from electron spectra and normalized to fit STAR measured data (from e-h correlation). The statistical errors are estimated for 100M 200 GeV Au+Au central events, shown in Figure 5.

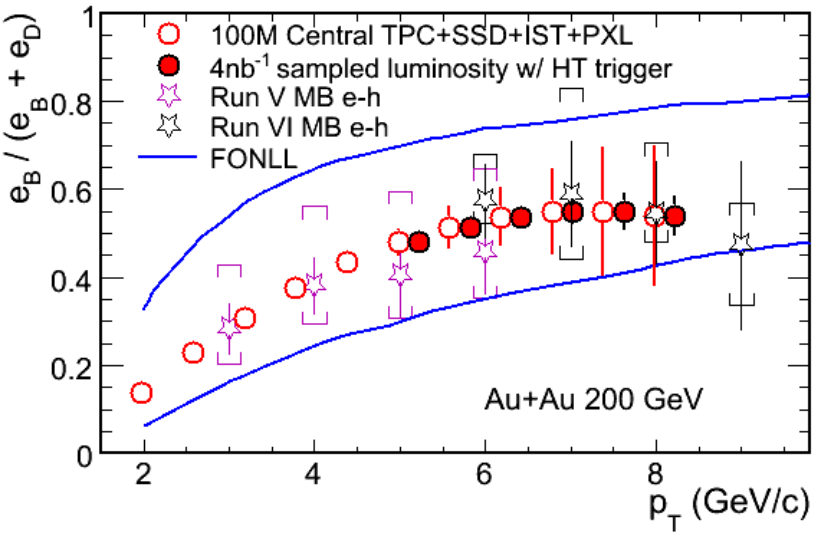

Figure 5: The (B→e)/NPE ratio as a function of p_T. Expected errors are estimated for 100M 200 GeV Au+Au central events (solid circles) and 4 nb^{-1} sampled luminosity with HT trigger (open circles).

The relative fractions of D→e and B→e can be varied by different cuts on electron DCA distributions. This can be used to measure electron v_2 for both D→e and B→e following the equation:

$$v_2^{NPE} = r \times v_2^{B\to e} + (1-r) \times v_2^{D\to e}, \qquad (1)$$

Here r is the (B→e)/NPE ratio. Table 2 shows two ratios from the two cases of different DCA cuts.

Case	Cut (μm)	e(D) eff. (%)	e(B) eff. (%)	r=e(B)/NPE
I	< 50	45.5	22.3	0.325
II	> 200	15.3	39.6	0.718

If we have the different v_2 measurements for total NPE from different DCA cuts, we can extract electron v_2 for both D→e and B→e. And we can also have precise measurement on D meson v_2 as a function of p_T via reconstruction from hadronic decay channel, which constrains the D→e v_2 due to decay kinematics. Thus, B→e v_2 can be obtained.

To estimate the electron v_2 statistics, we assume that D meson v_2 follows a cascade model with quark coalescence and does not drop at high p_T. The red curve in Figure 6 shows the D meson v_2 for the case that the charm quark has the same size partonic flow as measured for the light quarks ($v_{2c}=v_{2q}$). The blue curve shows the limiting case where the charm quark does not flow ($v_{2c}=0$). Then we use form factor decay to generate D→e v_2 distributions, shown as red open circles and blue open circles for the corresponding two cases. The ratio r=(B→e)/NPE is taken from STAR e-h correlation (Figure 5) and the total NPE v_2 is from PHENIX measurement. The B→e v_2 can be obtained from equation (1) shown as the red solid squares for the case of

v_{2c}=v_{2q} and the blue solid squares for the case of v_{2c}=0. The statistic errors are estimated for 500M 200 GeV Au+Au minimum bias events.

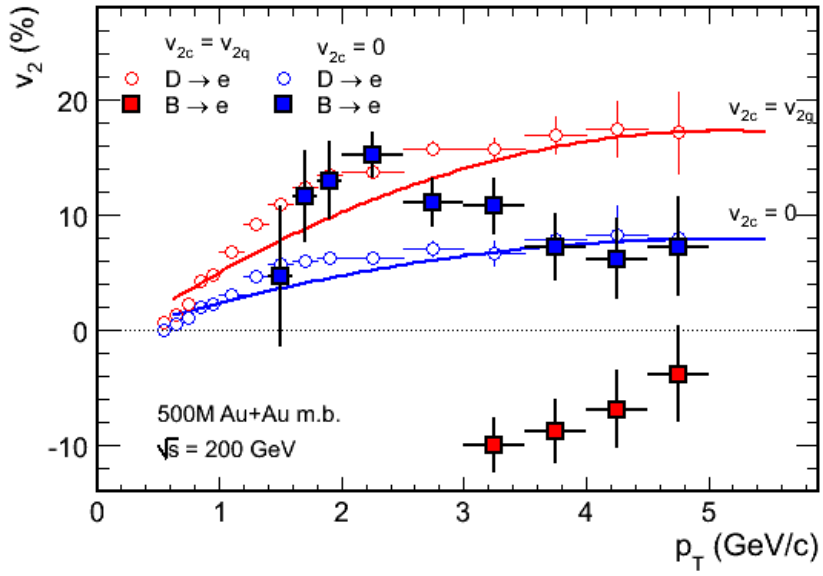

Figure 6: Expected errors of D→e and B→e v_2 for 500M 200 GeV Au+Au minimum bias events.